Published in final edited form as:
Am J Physiol Cell Physiol. 2003 February ; 284(2): C511–C520. doi:10.1152/ajpcell.00214.2002.

Mechanism of v-Src- and mitogen-activated protein kinase-induced reduction of gap junction communication

G. Trevor Cottrell[1], **Rui Lin**[2], **Bonnie J. Warn-Cramer**[2], **Alan F. Lau**[2], and **Janis M. Burt**[1]

[1]Department of Physiology, Arizona Health Sciences Center, University of Arizona, Tucson, Arizona 85724

[2]Cancer Research Center and Department of Cell and Molecular Biology, John A. Burns School of Medicine, University of Hawaii at Manoa, Honolulu, Hawaii 96813

Abstract

Connexin (Cx)43 gap junction channels are phosphorylated by numerous protein kinases, with the net effect typically being a reduction in gap junction communication (GJC). This reduction must result from a decrease in channel open probability, unitary conductance, or permselectivity, because previous results suggest that channel number is unaffected. Coexpression of v-Src with wild-type Cx43 (Cx43-wt) but not Cx43 with tyrosine to phenylalanine substitutions at 247 and 265 (Cx43-Y247,265F) resulted in reduced electrical and dye coupling but no change in single-channel amplitudes. EGF treatment of cells expressing Cx43-wt but not Cx43 with serine to alanine substitutions at 255, 279, and 282 (Cx43-S255,279,282A) resulted in reduced GJC, also with no change in single-channel amplitude. Dye coupling was reduced to a far greater extent than electrical coupling, suggesting that channel selectivity was also altered but with minimal effect on unitary conductance. The absence of Src- and MAPK-induced reductions in single-channel amplitude suggests that the decreases in GJC induced by these kinases result from reduced channel open probability and possibly altered selectivity.

Keywords

connexins; growth factors; dye permeability; electrophysiology; epidermal growth factor

Intercellular gap junctions are created by the aggregation of channels formed by the docking of two hexameric hemichannels. The integral gap junction proteins (connexins, Cx) belong to a relatively large gene family composed of at least 20 members in the human species. Nearly all gap junction channels permit the passage of ions, and some (e.g., Cx43) permit the passage of metabolites, secondary messengers, and other molecules of <1,000 Da. It is well established that direct cell-to-cell communication plays an important role in the growth of multicellular organisms. Cell survival in these organisms requires that each cell type retain its individuality while at the same time coordinating its activities with other neighboring cells. Gap junctions facilitate this by allowing intercellular communication to take place in a cell-specific and coordinated fashion (5).

Loss of gap junction communication (GJC) contributes to the transformed phenotype of many cancerous and precancerous cells (34). Furthermore, intracellular signaling cascades activated

Address for reprint requests and other correspondence: J. M. Burt, Dept. of Physiology, Arizona Health Sciences Center, Rm. 4103, Univ. of Arizona, Tucson, AZ 85724 (jburt@u.arizona.edu).

by numerous growth factors are known to decrease GJC (25), with these decreases being strongly correlated with phosphorylation of the Cx protein (11,33). Thus a major task in the gap junction research community is to identify the permeant molecules, determine their biological significance, and define the mechanisms for regulation of junctional permeability.

The mechanisms by which phosphorylation of Cx43 alter GJC are poorly understood. Electrical coupling between cells can be expressed as $g_j = N \cdot P_o \cdot \gamma_j$ where g_j is macroscopic electrical conductance, N is channel number, P_o is the open probability of the channels, and γ_j is their unitary conductance. Dye coupling (believed to be indicative of metabolic coupling) can be expressed in a similar manner as GJC = $N \cdot P_o \cdot$ Perm, where Perm reflects the permeability of the channel to the dye of interest, which can vary based on the dye's size, charge, and chemical composition. (These variations are indicative of channel selectivity.) Perm and γ_j both reflect the ease with which molecules move through the channel's pore. These equations predict that phosphorylation-induced decreases in g_j or GJC must result from decreases in one or more of the product factors.

Over two decades ago it was discovered that GJC is reduced between cells that express an activated temperature-sensitive mutant of the avian sarcoma virus (ts-Src) (3). Since then, numerous studies have identified the COOH-terminal tail of Cx43 protein as a target for tyrosine phosphorylation by v-Src and related protein tyrosine kinases (10–12,23,30), with v-Src being shown to directly interact with Cx43 through SH-2 and SH-3 binding domains (16, 24). Two tyrosine residues in the COOH terminus of wild-type Cx43 (Cx43-wt) have been determined to be crucial for v-Src binding, phosphorylation, and inhibition of GJC (22,30), although others have suggested that MAPK phosphorylation of serine residues may also be involved in v-Src-mediated decreases of GJC under acute treatment conditions (35).

The mechanism of GJC reduction in v-Src-stimulated, Cx43-expressing cells has not been examined in detail. Atkinson et al. (2) hypothesized that a decrease in channel N might account for the reduced coupling resulting from ts-Src activation. Contrary to expectation, their freeze-fracture analysis of gap junction plaques demonstrated that acute changes in ts-Src activity had no effect on junctional area at cell interfaces. Lin et al. (22) also found no evidence for change in Cx43-wt expression or immunofluorescence patterns in cells stably expressing v-Src. Together, these studies indicate that acute and steady-state v-Src activation do not influence channel N, and therefore must affect γ_j, permselectivity, or P_o. Moreno et al. (29) found a direct relationship between increased phosphorylation of Cx43-wt (by unknown kinases) and decreased γ_j. This finding was extended in studies of the PKC pathway, in which PKC activation increased the frequency of smaller subconductance events of Cx43-wt (19,21,28). In the typical setting where multiple gap junction channels are active and displaying multiple open states, P_o is not readily determined; therefore, to ascertain whether v-Src influences P_o, γ_j (or permselectivity) must be eliminated as a factor under the influence of v-Src.

Mechanisms of growth factor-mediated reduction of Cx43-wt GJC are greatly complicated by the numerous signaling cascades involved and possible cross talk between these cascades. As a result, rigorous investigation of the mechanisms of phosphorylation-induced reduction of GJC must be performed to delineate the effects of differing growth factor cascades on gap junction function. By using cell lines specifically engineered to explore the effects of v-Src and MAPK on Cx43-wt phosphorylation, we have tested the mechanisms by which these signaling cascades cause decreases in GJC. Unlike the PKC pathway, phosphorylation of Cx43-wt by Src (at tyrosines 247 and 265) or MAPK (at serines 255, 279, and 282) had no detectable effect on Cx43-wt channel γ_j, although the selectivity of these channels to different dyes was affected. Our data indicate that the decrease in electrical coupling induced by v-Src or MAPK was the result of channel closure (reduced P_o) whereas the decrease in GJC also involved increased channel selectivity.

MATERIALS AND METHODS

Cells and cell culture

The Cx43 knockout mouse cell line, −/−3 (26), expressing exogenous Cx43-wt (wtC1 clonal line), Cx43-wt and v-Src (wtS1 and wtS3 clonal lines), or the double mutant Cx43-Y247,265F (encoding phenylalanine substitutions at Y247 and Y265) and v-Src (dbS2 clonal line) (22) were used to assess mechanisms of v-Src-mediated reductions of GJC. The same knockout mouse cell line expressing the triple mutant Cx43-S255,279,282A (with serine to alanine substitutions at sites 255, 279 and 282; G11 cell line) (32) was used to assess mechanisms of MAPK-mediated reductions in GJC.

Cells were cultured in DMEM (D-1152; Sigma) supplemented with 10% FBS (Invitrogen) in a 5% CO_2 incubator at 37°C. Cell line stability was maintained by the presence of appropriate antibiotics at concentrations described previously (22,32). In studies with the Src kinase inhibitor PP2 (Biomol Research Laboratories), cells were incubated for 30 min in 10 μM PP2 at 25°C (6,13). To activate the MAPK pathway, cells were incubated for 20 min in 100 ng/ml EGF-rh (USB; Ref. 32).

Electrophysiology

The dual whole cell voltage-clamp technique was used to assess both macroscopic and single-channel conductance between pairs of cells in culture. Cells were grown to confluence in a 100-mm dish, lifted with 0.25% trypsin in Ca^{2+}- and Mg^{2+}-free buffer, and replated at low density on glass coverslips. Cells were allowed to adhere to the coverslips by incubating at 37° C for either 2–3 h, for single-channel recordings, or 24 h, for macroscopic conductance measurement.

Dual whole cell voltage-clamp experiments were carried out as previously reported (14,17). Glass electrodes were filled with one of two internal solutions. *Solution 1* (KCl) contained (in mM) 124 KCl, 14 CsCl, 9 HEPES, 9 EGTA, 0.5 $CaCl_2$, 5 glucose, 9 TEA-Cl, 3 $MgCl_2$, and 5 Na_2ATP, and *solution 2* (LKM) contained (in mM) 67.8 CsCl, 67.8 K-glutamate, 10 TEA-Cl, 0.5 $CaCl_2$, 3 $MgCl_2$, 5 glucose, 10 HEPES, 10 EGTA, and 5 Na_2ATP. *Solution 2* has lower bulk conductivity than *solution 1*, which results in lower unitary conductances for an equivalent channel population. The rationale for use of two different solutions was twofold: first, to mimic the previous electrophysiology performed on these same cells (21), and second, to increase the likelihood of a higher-resistance channel excluding or impeding the flow of larger ions between the cells, thereby enhancing the chances of observing conductance shifts in the presence of EGF. After the dual whole cell voltage-clamp configuration was achieved, both cells were held at 0 mV and then alternately stepped to −10 mV to measure macroscopic junctional conductance (g_j) and membrane conductance. Series resistance (R_s) was recorded for each cell with the capacitance compensation features of the Axopatch 1C amplifiers (Axon Instruments). Single-channel events were studied by reducing g_j to levels <0.5 nS with halothane (5 mM stock solution dripped into dish near cell pair) and recording single-channel activity with a transjunctional driving force of 40 mV. In only two experiments was g_j sufficiently low that halothane was not necessary for visualization of single-channel events.

Dye coupling studies

The extent of dye coupling was assessed using two separate dyes, Lucifer yellow [mol wt 443, net negative charge of 2, 5% (wt/vol)] and [2-(4-nitro-2, 1,3-benzoxadiol-7-yl)aminoethyl] trimethylammonium (NBD-TMA; mol wt 280, net positive charge of 1, 5 mM; kindly provided by Dr. Stephen Wright, University of Arizona, Tucson, AZ; see Ref. 4). Cells were grown to confluence on 25-mm glass coverslips. Injection electrodes (15–20 MΩ) were filled with dye by capillary action, backfilled with either 150 mM LiCl (for Lucifer yellow dye) or 200 mM

KCl (for NBD-TMA dye), and lowered onto the surface of the cell. Cells were impaled by the overcompensation of the capacitance feature of the amplifier (A-M Systems) and withdrawn after 10 s, and the cells receiving dye were determined after 1 min.

Data analysis

Single-channel records were analyzed with several strategies. The amplitudes of single-channel event transitions were manually determined. The minimum detectable difference between amplitudes was 0.25 pA, which corresponds to 6.25 pS at 40 mV transjunctional driving force. No binning of the data was performed. The frequency of events at each distinguishable current level was calculated as a percentage of the total number of events. The event data and event frequency data were used to construct histograms for each cell pair, and the data were fit (with Origin software) with one, two, or three Gaussian curves. The model resulting in the best fit was determined with the following criteria: *1*) standard deviations for the peak center parameters were <5% of the peak center value, and *2*) reduced χ^2 and R-squared values predicted significance at the $P < 0.05$ level. For each experimental group, the mean peak center values were compared by single-factor ANOVA or *t*-test as appropriate. All-points histograms were also generated from the digitized single-channel records with pCLAMP 8.1 (Axon Instruments) and Sigmaplot (SSPS). Event amplitudes determined directly from single-channel records and their corresponding all-points and event-frequency histograms were similar. Additionally, the percentage of total events in the 30-to 70-pS (*patch solution 1*)or 25- to 60-pS (*patch solution 2*) range was calculated for each experiment and treatment group and compared across treatment groups with a single-factorial ANOVA to assess whether v-Src or EGF treatment induced shifts of Cx43-wt channels to a lower conductance state.

The extent of dye coupling was determined as the total number of cells receiving dye from the injected cell after 1 min. The extent of coupling was compared for each dye across treatment groups with a single-factorial ANOVA. Tukey's honestly significant difference (HSD) test was used for post hoc comparisons. *t*-Tests were used to compare NBD-TMA vs. Lucifer yellow and NBD-TMA vs. NBD-TMA + PP2 within each treatment group. All statistical tests were deemed significant at $P < 0.05$.

RESULTS

Electrophysiology: junctional conductance

Relative to Cx43-wt expressing cells (wtC1 clone), electrical coupling was reduced in cells expressing v-Src with Cx43-wt (wtS1 and wtS3 clones) but not with Cx43-Y247,265F (dbS2 clone). Figure 1*A* presents uncorrected g_j and summed R_s values for the four cell types. Figure 1*B* presents the corrected [with the equations of van Rijen et al. (31)]g_j values. The wtC1 cells displayed a corrected g_j of 25.8 ± 3.7 nS ($n = 9$), whereas wtS1 and wtS3 cells had significantly less electrical coupling at 6.4 ± 2.3 ($n = 13$) and 13.7 ± 3.5 ($n = 12$) nS, respectively (Fig. 1*B*). The extent of coupling in dbS2 cells (27.6 ± 7.6 nS; $n = 9$) did not differ significantly from that in wtC1 cells, suggesting that the Cx43-Y247,265F mutations were sufficient to prevent significant electrical uncoupling by v-Src in these cells.

Electrical uncoupling of Cx43-wt- but not Cx43-S255,279,282A-expressing cells by EGF treatment was demonstrated previously, and therefore was not repeated here (32). Those data demonstrated that the S255,279,282A mutations were sufficient to prevent significant electrical uncoupling by EGF.

Electrophysiology: unitary conductance

Single-channel records from Cx43-wt-expressing wtC1 cells revealed predominantly 90- to 110-pS events (Fig. 2*A*), although smaller events in the range of 30–70 pS were observed in

most cell pairs. Peak-to-peak separation on the corresponding all-points histogram confirmed a main-state conductance of ~100 pS and a substate conductance of ~60 pS. The amplitudes of 210 events from this cell pair (86 s of record) were used to construct an event-frequency histogram that was best fit with two peaks (Fig. 2*E*) with conductances corresponding to 93 ± 0.3 pS (SD) and 51 ± 1.2 pS (SD). Data from only three of six cell pairs were best fit with two peaks; the remaining cell pairs were best fit with only one peak. Across six cell pairs, the mean mainstate conductance was 94 ± 1.6 pS (SE); for the three pairs whose data were best fit by two peaks the mean conductance of the substate was 47 ± 2.5 pS.

In cells coexpressing v-Src with Cx43-wt (wtS1 and wtS3 cell lines) a comparable distribution of event amplitudes was observed, with 85- to 120-pS events predominating and smaller events occurring at a lower frequency. Figure 2, *B* and *C* , illustrates examples that represent the extremes of the range of channel behavior observed in the presence of v-Src. Consistent with the amplitudes evident in the single-channel records and corresponding all-points histograms, the event-frequency histograms for the illustrated cell pairs (263 events from 416 s and 297 events from 246 s, respectively) were best fit with two peaks with conductances corresponding to 87 ± 0.81 and 48 ± 1.2 pS for the wtS1 pair (Fig. 2*F*) and 115 ± 1 and 66 ± 1.4 pS for the wtS3 pair (Fig. 2*G*). Across five cell pairs in each group, the mean main-state conductance was 100 ± 10 and 107 ± 6 pS (SE) for the S1 and S3 pairs, respectively. The event-frequency data from only two of five wtS1 pairs and four of the five wtS3 pairs were best fit by two peaks—the conductance of this second peak was 59 ± 3.5 pS ($n = 6$).

dbS2 cell pairs were almost identical to wtC1 cell pairs, with 90- to 110-pS events predominating (Fig. 2*D*). The all-points histogram and event-frequency histogram (Fig. 2*H*) for this cell pair indicated the presence of a main-state conductance of 89 ± 0.73 pS. Although smaller events were observed in this and other dbS2 cell pairs, the data from only one of five pairs were best fit by two peaks. The main-state conductance across multiple dbS2 pairs ($n = 5$) was 98 ± 3.6 pS.

The conductances of the main state and substate observed in wtC1, wtS1, wtS3, and dbS2 pairs were not statistically different (ANOVA; $P > 0.38$). Because smaller events were observed in pairs whose data were not best fit by two peaks, we calculated the frequency of events in the 30- to 70-pS range for each pair in each experimental group, calculated the means for each group, and statistically compared the means for differences. No differences between groups were observed (frequency of 30- to 70-pS events expressed as % of total events: wtC1 = 21.6 ± 7.9, wtS1 = 19.2 ± 8.4, wtS3 = 29.3 ± 8, dbS2 = 20 ± 14.4). The predominance of 80- to 120-pS single-channel events (main-state dominance) combined with no significant differences in smaller channel event amplitude or frequency (30–70 pS) indicate that the vSrc-induced reduction in GJC observed in v-Src-transfected cells was not attributable to reduced γ_j in these cells.

Treatment of wtC1 (Fig. 3*A*) cells with 100 ng/ml EGF (Fig. 3*B*) did not cause any notable shifts in single-channel behavior. Comparison of single-channel records and the corresponding all-points and event-frequency histograms (Fig. 3, *C* and *D*) obtained from cell pairs in the absence and presence of EGF revealed in both cases predominantly 70- to 100-pS channel events. Smaller events, in the 25- to 60-pS range, were observed when EGF was absent but rarely seen when EGF was present. Data from three of six pairs were best fit with two peaks under control conditions, whereas the data from zero of five pairs treated with EGF were best fit with two peaks. Main-state conductances were 90 ± 3 and 88 ± 7 pS in the absence and presence of EGF, respectively. The percentage of total events in the 25- to 60-pS range also did not differ in the EGF-treated and control groups (control: 24 ± 11%; EGF: 5 ± 5%).

EGF also had no effect on event amplitude or frequency in the Cx43-S255,279,282A-expressing G11 cells. Single-channel records with the corresponding all-points histograms (Fig. 4, *A* and *B*) and event-frequency histograms (Fig. 4, *C* and *D*) all indicated the presence of a main-state conductance of 75 ± 1pS in both the presence and absence of EGF (n = 6 for both conditions). In both cases smaller events were occasionally observed, and in both groups the data from one cell pair were best fit with two peaks. The percentage of total events with amplitudes in the 25- to 60-pS range in control and treatment groups was not different (16 ± 5% and 14 ± 8%, respectively). These results indicate that the EGF-induced reduction in junctional conductance observed in control cells did not result from a reduction in event amplitude. No unitary conductance changes were measured between treatment conditions; therefore the loss of g_j previously observed for similar EGF-treated cells (32) was not the result of a shift in single-channel conductance to a lower conductance state.

GJC and junctional selectivity

The introduction of negatively charged inorganic phosphate moieties to the COOH terminus of Cx43 could shift gap junction channel selectivity toward preferential cation transfer. The dye Lucifer yellow has two negative charges at physiological pH; therefore, its transfer may not be favored through phosphorylated Cx43 gap junction channels. Here we used both Lucifer yellow and the novel cationic dye NBD-TMA (9) to assess the impact of Src and EGF on GJC and junctional selectivity. In addition, the v-Src inhibitor PP2 was used to ensure that the differences in dye coupling between cell types resulted from v-Src and not chance clonal differences between cell populations.

GJC was evaluated as extent of coupling, calculated as the total number of cells to which dye diffused within 1 min after injection. In wtC1 cells, NBD-TMA coupling was greater than Lucifer yellow coupling (13.7 ± 1.4 vs. 7.2 ± 0.8; Fig. 5*A*) and was significantly increased after PP2 treatment (18.6 ± 1.9 vs. 13.7 ± 1.4), perhaps reflecting the effects of basal c-Src activity. Lucifer yellow coupling was nearly absent, and NBD-TMA coupling was reduced from 13.7 cells to 0.2 ± 0.09 and 0.65 ± 0.28 cells in the wtS1 and wtS3 cells, respectively. After PP2 treatment, NBD-TMA coupling in wtS1 and wtS3 cells was significantly improved although still not equal to that of wtC1 cells. Extent of coupling in the Cx43-Y247,265F-expressing dbS2 cells was comparable for Lucifer yellow (5 ± 1 cells) and NBD-TMA (with PP2 pretreatment: 5 ± 1 cells; without PP2 pretreatment: 6 ± 1 cells) and well below that observed for the wtC1 cells. The lower levels of coupling in dbS2 compared with wtC1 cells most likely reflected differing growth morphologies of the dbS2 cells—they do not form confluent monolayers like wtC1 cells. EGF treatment of wtC1 cells resulted in a significant decrease in Lucifer yellow (0.33 ± 0.17) (15,32) and NBD-TMA (0.88 ± 0.26) transfer. These results are consistent with the junctional conductance data in that both types of data indicate that Src and MAPK reduce GJC.

To evaluate whether Src or MAPK alters junctional selectivity, the decreases in junctional conductance (electrical coupling) of wtS1, wtS3, and EGF-treated wtC1 cells were computed relative to wtC1 cells and used to predict “expected” levels of NBD-TMA and Lucifer yellow dye coupling (Fig. 5*B*). Junctional conductance in wtS1, wtS3, and EGF-treated wtC1 cells was 25%, 53%, and 43% of that observed in wtC1 cells. If NBD-TMA coupling were reduced to the same extent, these values predict NBD-TMA coupling levels in these groups of 3.4, 7.2, and 5.8 cells, respectively. The observed values were significantly lower at 0.2, 0.65, and 0.9 cells. Extent of Lucifer yellow coupling (0, 0.05, and 0.33) was also less than the junctional conductance values predicted (1.8, 3.8, and 3.1 cells) for the wtS1, wtS3, and EGF-treated wtC1 cell populations.

If the channel displayed no charge- or size-based differences in selectivity, then the relative decrease in the extent of coupling for NBD-TMA and Lucifer yellow would be similar in

response to v-Src or MAPK. The decreases in NBD-TMA coupling of wtS1, wtS3, and EGF-treated wtC1 cells were computed relative to the wtC1 cells and used to predict expected levels of Lucifer yellow dye coupling in the wtS1, wtS3, and EGF-treated wtC1 cells. The observed values of 0, 0.05, and 0.33 cells were considerably less than the predicted values of 0.11, 0.34, and 0.46 cells, respectively (Fig. 5*B*). These comparisons suggest that Src and MAPK alter the selectivity of Cx43-wt channels such that the reduction in electrical coupling is far less than that for dye coupling, with additional dye-dependent differences.

DISCUSSION

A decrease in GJC or electrical coupling must involve a decrease in channel *N*, P_o, γ_j, permselectivity, or a combination of these factors. We have demonstrated that the previously reported v-Src- and MAPK-induced decreases in Cx43-mediated electrical coupling occur independent of a decrease in the unitary conductance of the channel. Because Cx43 expression and localization are also not affected by v-Src (2,22) or MAPK (32) activation, the observed decreases in electrical coupling must reflect decreased channel P_o. We have further demonstrated that v-Src and MAPK activation reduced GJC and have shown that the magnitudes of the decreases for the two dyes were not predicted well by the observed decreases in electrical coupling. These results suggest that Src and MAPK alter channel selectivity. These findings contrast with findings for the PKC pathway, in which PKC-mediated phosphorylation induces a decrease in junctional conductance that can be at least partially attributed to a decrease in channel unitary conductance (21).

The absence of a reliable measure for P_o in cell pairs coupled by multiple gap junction channels limits our analysis of gating mechanisms. The presence in most junctions of several channels, each with multiple possible conductance states, complicates any analysis of P_o. A simultaneous decrease in main-state P_o and increase in substate P_o, in combination with possible changes in channel *N*, make P_o-based interpretations of changes in g_j challenging at best. An example of this is described by Kwak et al. (19), who found that g_j increased despite decreased predominance of large γ_j events. Apparently, the increased predominance of the substate conductance was accompanied by either an increased P_o of that channel state or an increased channel *N*.

In the absence of P_o data, it is necessary to eliminate the other factors that contribute to GJC as potential candidates for v-Src- and MAPK-mediated reductions in GJC. Early studies of v-Src effects on GJC used a temperature-sensitive v-Src mutant that was activated by shifting cells in culture from a nonpermissive temperature of 40°C to a permissive temperature of 35° C (2,3). These experiments permitted the measurement of GJC and gap junction size, an indicator of gap junction channel *N*, after chronic (>12 h) or acute (<60 min) activation of v-Src. Chronic growth of cells at the permissive temperature resulted in a loss of GJC compared with cells grown at the nonpermissive temperature. Similarly, acutely shifting cells to and from the permissive temperature resulted in loss and gain of GJC, respectively. Measurements of gap junction area per interface demonstrated that chronic growth of cells at the permissive temperature resulted in a decreased gap junction area. However, this effect could not be attributed to the action of v-Src, because nontransfected (with vSrc) cells grown at 35 °C also had a decreased plaque area compared with those grown at 40°C. In addition, acute shifts between the nonpermissive and permissive temperatures had no effect on gap junction area despite changes in GJC. These data indicate that the Src-induced decrease in GJC did not result from decreased channel *N*. Using Western blots, Lin et al. (22) found comparable Cx43 expression levels in wtC1, wtS1, and dbS2 cells, with no apparent differences in Cx43 localization observed after immunofluorescent labeling, lending further support to the conclusion that v-Src can cause decreased GJC without reducing channel *N*. Neither measure of channel *N*, morphological or biochemical, provides information on the functionality of the

channels. Regardless of whether channel *N* differs between the wtC1 and wtS1 or wtS3 cell lines, our PP2 and EGF data, which explore the acute effects of v-Src inhibition and MAPK activation, strongly suggest that these kinases modify channel gating. These observations, combined with the absence of differing expression levels and localization of Cx43 between cell types (22) and the absence of change in gap junction area in v-Src-treated cells (2), argue strongly that the loss of GJC measured in our v-Src-transfected cells are not the result of decreased channel *N*.

Cx43 characteristically has three open conformations: the main state with a typical conductance of ~100 pS (dependent on pipette solutions used), a substate with a conductance of ~60 pS, and a residual state with a conductance of ~30 pS. Transitions between the ground state (fully closed) and each of these open conformations can be observed. As well, transitions can be observed from the main state to a residual state. The 60-pS substate appears to be favored when the channel is phosphorylated (19,29), but the prevalence of ~60-pS transitions between the main state and residual state complicates interpretation of such data.

Recent studies comparing behavior of Cx43-wt and mutant (Cx43-S368A) isoforms have strengthened the conclusion that phosphorylation can induce changes in channel unitary conductance (21). Phosphorylation of Cx43 by PKC induces a dramatic increase in prevalence of the 60-pS substate and decrease in prevalence of the main state. These changes in channel behavior likely contribute to the decrease in GJC induced during PKC activation, but simultaneous changes in P_o and *N* may also occur. Decreases in unitary conductance result from increasing the channel's pore length, increasing selectivity to current-carrying ions, increasing access resistance, decreasing pore diameter, or a combination of these effects. Phosphorylation of Cx43 by PKC therefore may induce a conformational change at the Cx43 COOH terminus that acts to partially occlude or lengthen the channel pore, increase its selectivity, or increase access resistance to the pore. In contrast to these results with PKC, the unitary conductance profile of Cx43 was not altered by v-Src or MAPK activation. Phosphorylation of Cx43 by PKC takes place at serine 368, a site close to the end of the COOH-terminal tail, whereas v-Src and MAPK induce phosphorylation of Cx43 at the proximal end of the COOH-terminal region (amino acid residues 247–282). Differing effects of phosphorylation in proximal vs. distal regions of the COOH terminus may suggest differing roles for these regions.

It is reasonable to hypothesize that phosphorylation of the COOH-terminal tail of Cx43 could alter channel selectivity or access resistance. The introduction of negatively charged moieties at the entry to the pore region of the gap junction channel could act to selectively draw cations through the channel while impeding the progress of anions. Our data suggest that if such changes in selectivity are occurring, their impact on electrical vs. dye coupling are quite different. The γ_j of channels observed in the presence of v-Src and activated MAPK were not different, suggesting that the decrease in electrical coupling was due to a decrease in P_o. If this were the only effect of these kinases, one might expect dye coupling to decrease in parallel to the decrease in junctional conductance. Such was not the case. Lucifer yellow dye coupling was reduced to a far greater extent than NBD-TMA dye coupling, and the latter was reduced to a far greater extent than would be predicted by changes in junctional conductance in wtS1, wtS3, and EGF-treated wtC1 cells. These results suggest that selectivity of the channel was affected by these treatments but in a fashion that was undetectable relative to γ_j. This suggestion merits further attention in experiments that measure g_j and dye diffusion simultaneously, an approach beyond the scope of the current study.

Considerable debate surrounds the mechanistic basis of v-Src-mediated reduction of GJC. Although v-Src activity has been associated with increased predominance of phosphoserines and phosphotyrosines on Cx43, decreases in GJC were most commonly associated with

tyrosine phosphorylation (10–12,23). Swenson et al. (30) demonstrated that v-Src decreased GJC of Cx43 by phosphorylation of Tyr265. Lin et al. (22) corroborated these results and determined that Tyr247 phosphorylation was also involved. In contrast, Zhou et al. (35) determined that Tyr247 and Tyr265 were not required for v-Src-mediated gating of Cx43. Instead, they provided evidence that MAPK phosphorylation of serines 255, 279, and 282 was necessary. In their model, they transfected *Xenopus* oocytes with Cx43 cRNA, permitted channels to form, and then injected v-Src cRNA to induce uncoupling. This differs from the other studies that chronically coexpressed v-Src and Cx43 (22,30). It is possible that acute activation of v-Src has different effects on MAPK activity than chronic v-Src presence. In the stably transfected v-Src cells, the constant presence of Src activity may result in negative-feedback regulation of elements of the MAPK cascade, thus decreasing the sensitivity of this cascade to v-Src activation. If this were true, then the role that MAPK may play in v-Src-induced gating of Cx43 channels would be greatly diminished in the chronically active v-Src cell model. The possibility of cross talk between these signaling cascades prompted us to investigate the mechanisms of MAPK-induced decreases in GJC in conjunction with v-Src gating mechanisms. As stated previously, no differences were observed.

It is clear that regulation of gap junctions by growth factor-mediated signaling cascades is complicated. We have shown here that mechanisms of growth signaling-mediated decreases in GJC caused by v-Src and MAPK are different from those previously described for PKC activation (21) and that this is the result of specific phospho-amino acid residue localization in the COOH terminus. Although regulation of Cx43 by growth signaling cascades is most commonly studied, many other connexins are considered phosphoproteins as well (for review see Ref. 20), and these connexins can be differentially regulated by similar phosphorylating conditions (18). Furthermore, two different cell types expressing similar connexins may not have the same GJC response to a signal cascade agonist (1). These issues have been further complicated by the ability of connexins to form heteromeric/heterotypic channels (8) and the possibility that Cx hemichannels may also be regulated by growth signaling (7) and that gap junction proteins may influence growth independently from their formation of functional channels (27).

Such complexities make it essential to develop an understanding of relationships between phosphorylation of Cx43 and the impact that this can have on gap junction channel function. We provide evidence here that Cx43 phosphorylation can acutely alter electrical coupling through changes in P_o, independent of changes in γ_j. Concomitant changes in GJC likely involve enhanced permselectivity as well as reduced P_o. The overall effect that this has on cell physiology is not understood; however, mechanistic understanding of channel phosphorylation provides a starting point for the study of the physiological impacts that these changes will have at the cellular level.

Acknowledgments

This work was supported in part by National Institutes of Health Grants HL-58732 to J. M. Burt and CA-52098 to A. F. Lau.

REFERENCES

1. Albright CD, Grimley PM, Jones RT, Resau JH. Differential effects of TPA and retinoic acid on cell-cell communication in human bronchial epithelial cells. Exp Mol Pathol 2002;72:62–67. [PubMed: 11784124]
2. Atkinson MM, Anderson SK, Sheridan JD. Modification of gap junctions in cells transformed by a temperature-sensitive mutant of Rous sarcoma virus. J Membr Biol 1986;91:53–64. [PubMed: 3016281]

3. Atkinson MM, Menko AS, Johnson RG, Sheppard JR, Sheridan JD. Rapid and reversible reduction of junctional permeability in cells infected with a temperature-sensitive mutant of avian sarcoma virus. J Cell Biol 1981;91:573–578. [PubMed: 6273447]
4. Bednarczyk D, Mash EA, Aavula BR, Wright SH. NBD-TMA: a novel fluorescent substrate of the peritubular organic cation transporter of renal proximal tubules. Pflügers Arch 2000;440:184–192.
5. Bruzzone R, White TW, Paul DL. Connections with connexins: the molecular basis of direct intercellular signaling. Eur J Biochem 1996;238:1–27. [PubMed: 8665925]
6. Chen JK, Capdevila J, Harris RC. Overexpression of C-terminal Src kinase blocks 14,15-epoxyeicosatrienoic acid-induced tyrosine phosphorylation and mitogenesis. J Biol Chem 2000;275:13789–13792. [PubMed: 10788500]
7. Contreras JG, Sanchez HA, Eugenin EA, Speidel D, Theis M, Willecke K, Bukauskas F, Bennet MVL, Saez JC. Metabolic inhibition induces opening of unapposed connexin 43 gap junction hemichannels and reduces gap junctional communication in astrocytes in culture. Proc Natl Acad Sci USA 2002;99:495–500. [PubMed: 11756680]
8. Cottrell GT, Burt JM. Heterotypic gap junction channel formation between heteromeric and homomeric Cx40 and Cx43 connexons. Am J Physiol Cell Physiol 2001;281:C1559–C1567. [PubMed: 11600419]
9. Cottrell GT, Wu Y, Burt JM. Cx40 and Cx43 expression ratio influences heteromeric/heterotypic gap junction channel properties. Am J Physiol Cell Physiol 2002;282:C1469–C1483. [PubMed: 11997262]
10. Crow DS, Beyer ES, Paul DL, Kobe SS, Lau AF. Phosphorylation of Connexin43 gap junction protein in uninfected and rous sarcoma virus-transformed mammalian fibroblasts. Mol Cell Biol 1990;10:1754–1763. [PubMed: 1690850]
11. Crow DS, Kurata WE, Lau AF. Phosphorylation of connexin43 in cells containing mutant src oncogenes. Oncogene 1992;7:999–1003. [PubMed: 1315016]
12. Goldberg GS, Lau AF. Dynamics of connexin43 phosphorylation in $pp60^{v\text{-}src}$-transformed cells. Biochem J 1993;295:735–742. [PubMed: 7694570]
13. Hanke JH, Gardner JP, Dow RL, Changelian PS, Brissette WH, Weringer EJ, Pollok BA, Connelly PA. Discovery of a novel, potent, and Src family-selective tyrosine kinase inhibitor. Study of Lck- and FynT-dependent T cell activation. J Biol Chem 1996;271:695–701. [PubMed: 8557675]
14. He DS, Jiang JX, Taffet S, Burt JM. Formation of heteromeric gap junction channels by connexins 40 and 43 in vascular smooth muscle cells. Proc Natl Acad Sci USA 1999;96:6495–6500. [PubMed: 10339616]
15. Kanemitsu MY, Lau AF. Epidermal growth factor stimulates the disruption of gap junctional communication and connexin43 phosphorylation independent of 12-*O*-tetradecanoylphorbol 13-acetate-sensitive protein kinase C: the possible involvement of mitogen-activated protein kinase. Mol Biol Cell 1993;4:837–848. [PubMed: 8241569]
16. Kanemitsu MY, Loo LW, Simon S, Lau AF, Eckhart W. Tyrosine phosphorylation of connexin 43 by v-Src is mediated by SH2 and SH3 domain interactions. J Biol Chem 1997;272:22824–22831. [PubMed: 9278444]
17. Kurjiaka DT, Steele TD, Olsen MV, Burt JM. Gap junction permeability is diminished in proliferating vascular smooth muscle cells. Am J Physiol Cell Physiol 1998;275:C1674–C1682.
18. Kwak BR, Hermans MMP, De Jonge HR, Lohmann SM, Jongsma HJ, Chanson M. Differential regulation of distinct types of gap junction channels by similar phosphorylating conditions. Mol Biol Cell 1995;6:1707–1719. [PubMed: 8590800]
19. Kwak BR, Van Veen TAB, Analbers LJS, Jongsma HJ. TPA increases conductance but decreases permeability in neonatal rat cardiomyocyte gap junction channels. Exp Cell Res 1995;220:456–463. [PubMed: 7556455]
20. Lampe PD, Lau AF. Regulation of gap junctions by phosphorylation of connexins. Arch Biochem Biophys 2000;384:205–215. [PubMed: 11368307]
21. Lampe PD, Tenbroek E, Burt JM, Kurata WE, Johnson RG, Lau AF. Phosphorylation of connexin43 on serine368 by protein kinase C regulates gap junctional communication. J Cell Biol 2000;149:1503–1512. [PubMed: 10871288]
22. Lin R, Warn-Cramer BJ, Kurata WE, Lau AF. v-Src phosphorylation of connexin 43 on Tyr247 and Tyr265 disrupts gap junctional communication. J Cell Biol 2001;154:815–827. [PubMed: 11514593]

23. Loo LWM, Berestecky JM, Kanemitsu MY, Lau AF. pp60^{src}-mediated phosphorylation of connexin 43, a gap junction protein. J Biol Chem 1995;270:12751–12761. [PubMed: 7539006]
24. Loo LWM, Kanemitsu MY, Lau AF. In vivo association of pp60$^{v\text{-}src}$ and gap-junction protein connexin 43 in *v-src*-transformed fibroblasts. Mol Carcinog 1999;25:187–195. [PubMed: 10411145]
25. Maldonado PE, Rose B, Loewenstein WR. Growth factors modulate junctional cell-to-cell communication. J Membr Biol 1988;106:203–210. [PubMed: 2854164]
26. Martyn KD, Kurata WE, Warn-Cramer BJ, Burt JM, Tenbroek E, Lau AF. Immortalized connexin43 knockout cell lines display a subset of biological properties associated with the transformed phenotype. Cell Growth Differ 1997;8:1015–1027. [PubMed: 9300183]
27. Moorby C, Patel M. Dual functions for connexins: Cx43 regulates growth independently of gap junction formation. Exp Cell Res 2001;271:238–248. [PubMed: 11716536]
28. Moreno AP, Campos de Carvalho AC, Christ G, Melman A, Spray DC. Gap junctions between human corpus cavernosum smooth muscle cells: gating properties and unitary conductance. Am J Physiol Cell Physiol 1993;264:C80–C92.
29. Moreno AP, Saez JC, Fishman GI, Spray DC. Human connexin43 gap junction channels: regulation of unitary conductances by phosphorylation. Circ Res 1994;74:1050–1057. [PubMed: 7514508]
30. Swenson KI, Piwnica-Worms H, McNamee H, Paul DL. Tyrosine phosphorylation of the gap junction protein conexin43 is required for the pp60$^{v\text{-}src}$-induced inhibition of communication. Cell Regul 1990;1:989–1002. [PubMed: 1966893]
31. Van Rijen HV, Wilders R, Van Ginneken AC, Jongsma HJ. Quantitative analysis of dual whole-cell voltage-clamp determination of gap junctional conductance. Pflügers Arch 1998;436:141–151.
32. Warn-Cramer BJ, Cottrell GT, Burt JM, Lau AF. Regulation of connexin43 gap junctional intercellular communication by mitogen-activated protein kinase. J Biol Chem 1998;273:9188–9196. [PubMed: 9535909]
33. Warn-Cramer BJ, Lampe PD, Kurata WE, Kanemitsu MY, Loo LWM, Eckhart W, Lau AF. Characterization of the mitogen-activated protein kinase phosphorylation sites on the connexin43 gap junction protein. J Biol Chem 1996;271:3779–3786. [PubMed: 8631994]
34. Yamasaki H, Hollstein M, Mesnil M, Martel N, Aguelon AM. Selective lack of intercellular communication between transformed and nontransformed cells as a common property of chemical and oncogene transformation of BALB/c 3T3 cells. Cancer Res 1987;47:5658–5664. [PubMed: 3311356]
35. Zhou L, Kasperek EM, Nicholson BJ. Dissection of the molecular basis of pp60$^{v\text{-}src}$ induced gating of connexion 43 gap junction channels. J Cell Biol 1999;144:1033–1045. [PubMed: 10085299]

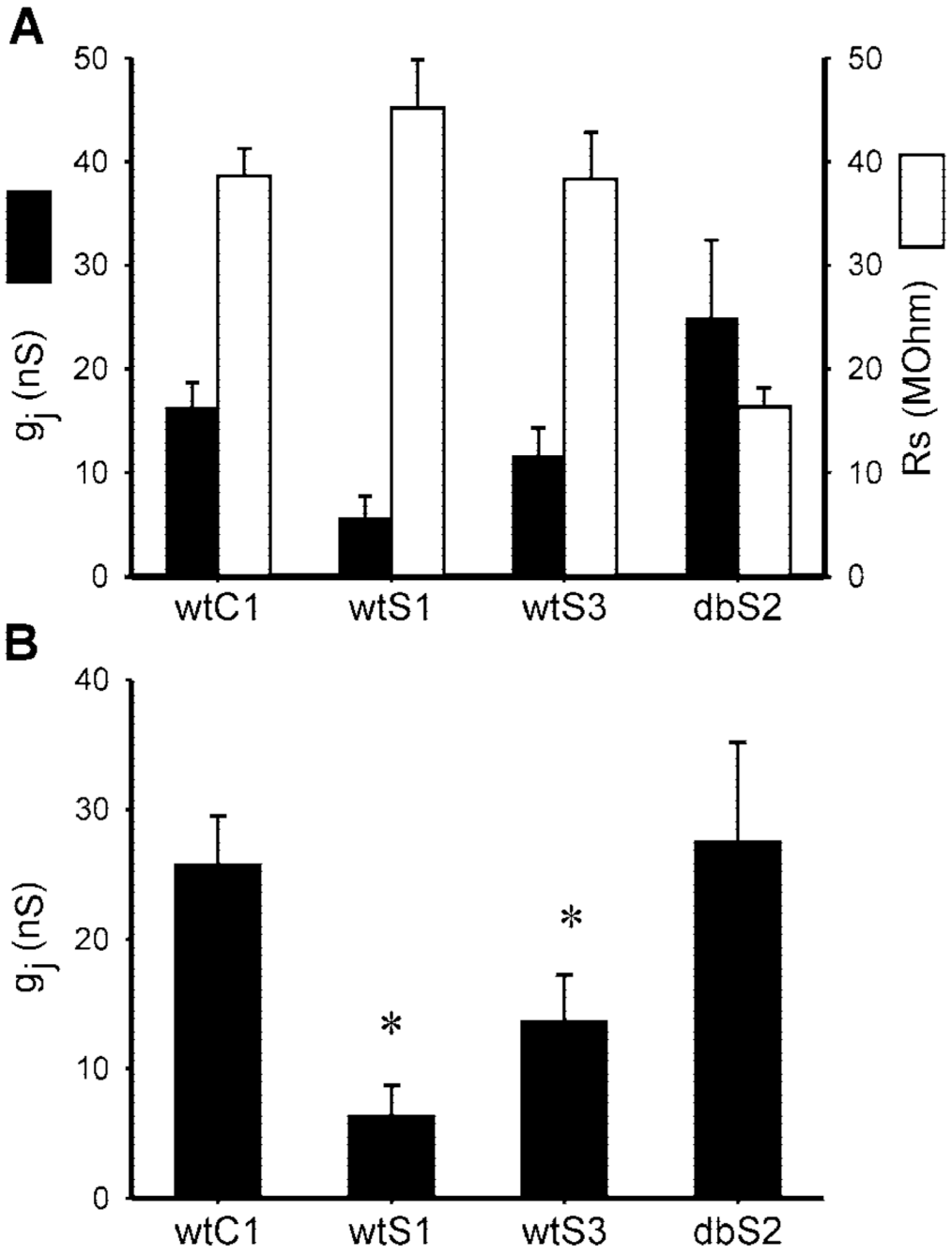

Fig. 1.

Macroscopic junctional conductance after 24 h of plating.*A*: uncorrected mean macroscopic electrical conductance (g_j) measurements (filled bars) with corresponding mean series resistance (R_s) values (open bars) for wtC1 [wild-type connexin (Cx)43 (Cx43-wt); $n = 9$], wtS1 (Cx43-wt and v-Src; $n = 13$), wtS3 (Cx43-wt and v-Src; $n = 12$), and dbS2 [Cx 43 with Y to F substitutions at 247, 265 (Cx43-Y247,265F) and v-Src; $n = 9$]cell pairs. B: corrected mean g_j values for each cell type. v-Src expression was sufficient to reduce g_j in wtS1 and wtS3 cells. *Significant difference from wtC1 ($P < 0.05$).

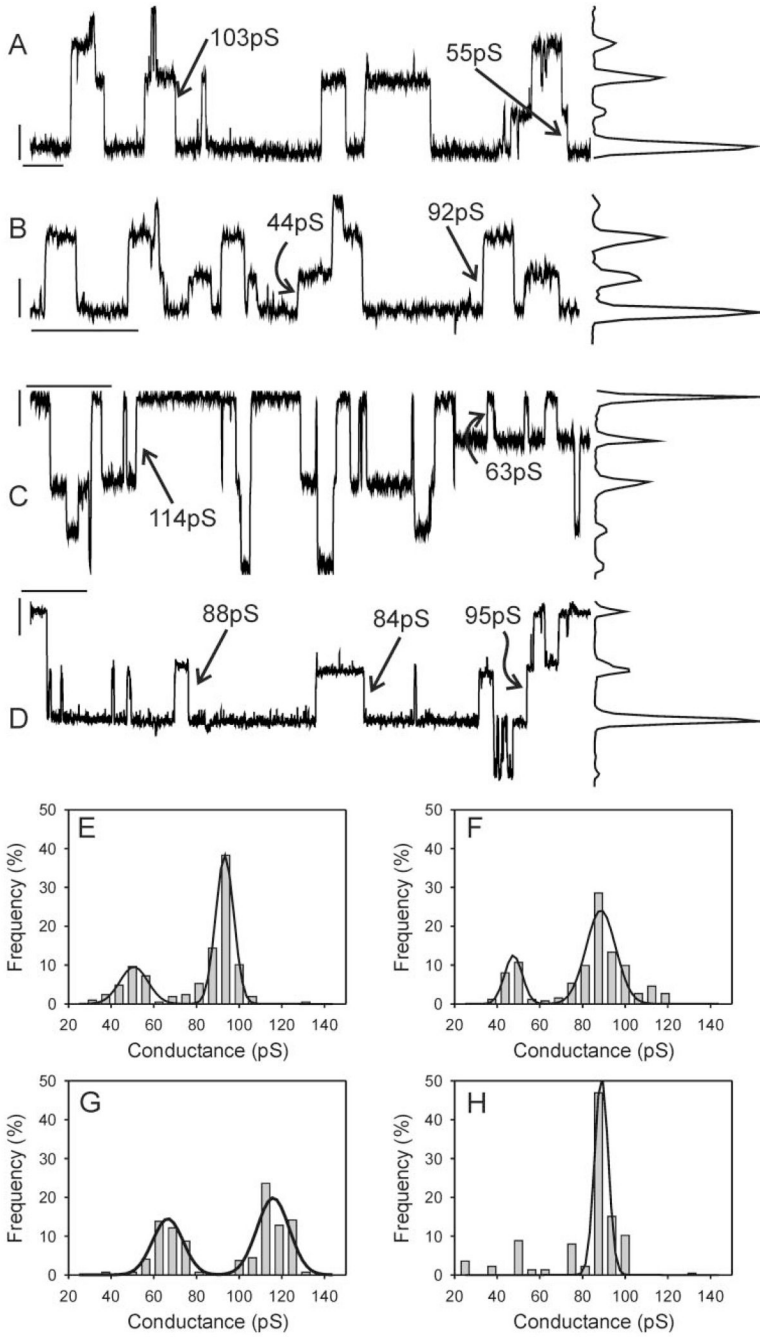

Fig. 2.

Single-channel records with corresponding all-points histograms (*A–D*) and event-frequency histograms (*E–H*) derived from wtC1 (*A*, *E*), wtS1 (*B*, *F*), wtS3 (*C*, *G*), and dbS2 (*D*, *H*). In all cases halothane was used to reduce junctional conductance (P_o effect) to a level at which single-channel events could be discerned. Transjunctional driving force was 40 mV, and records were notch filtered and low-pass filtered at 100 Hz (8-pole Bessel). Calibration bars in *A–D* correspond to 2 pA and 2 s and are located near the zero transjunctional current level. Data from multiple cell pairs similarly analyzed indicated that no significant differences in channel amplitude existed between treatment groups (see text).

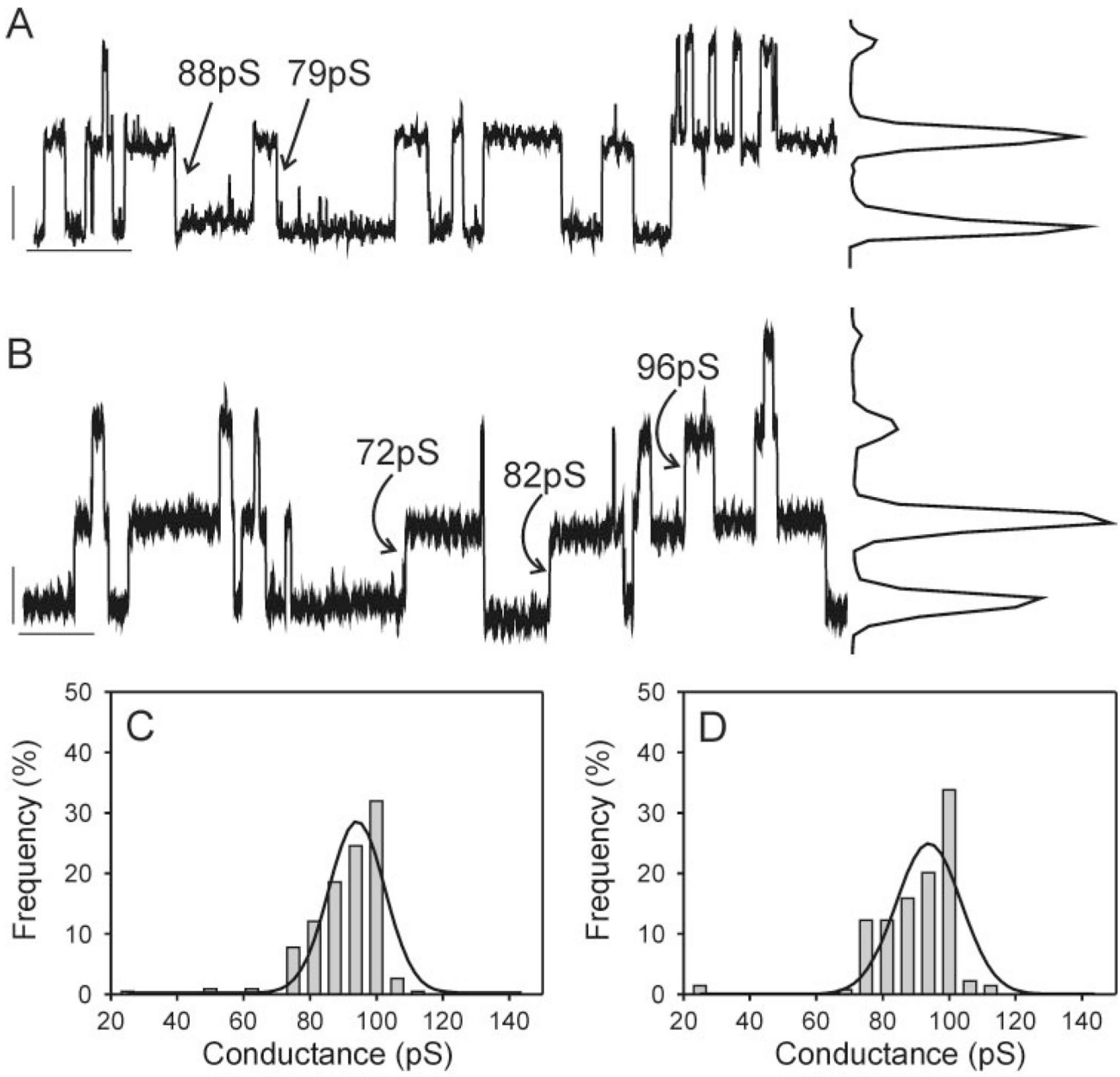

Fig. 3.

Single-channel records with corresponding all-points histograms (*A*, *B*) and event-frequency histograms (*C*, *D*) derived from wtC1 cells in the absence (*A*, *C*) and presence (*B*, *D*)of 100 ng/ml EGF. Records were notch filtered and low-pass filtered at 100 Hz (8-pole Bessel). Calibration bars in *A* and *B* correspond to 2 pA and2sand are located near the zero current level. Note the absence of any differences in channel amplitude in the presence vs. absence of EGF.

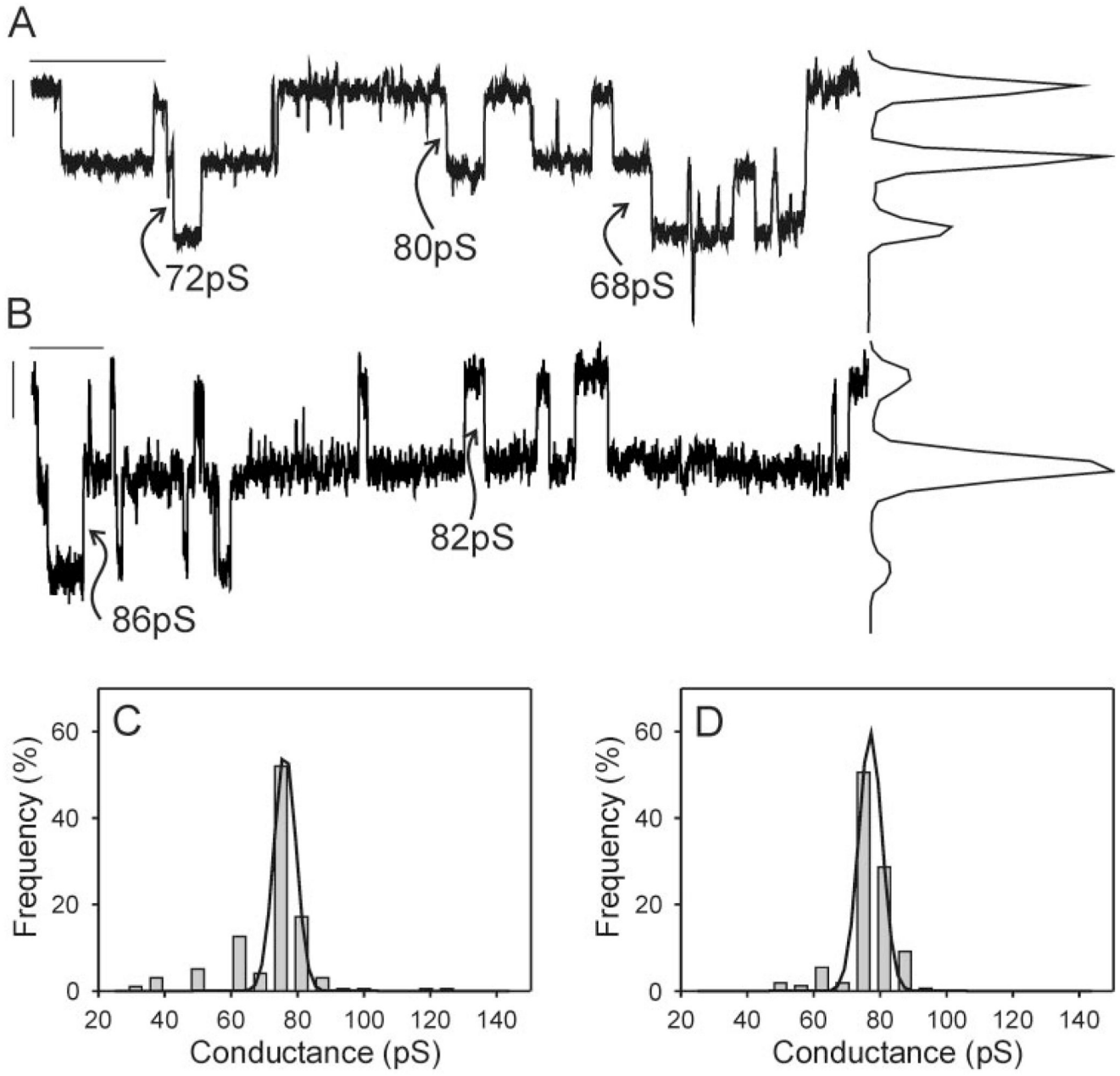

Fig. 4.

Single-channel records with corresponding all-points histograms (*A*, *B*) and event-frequency histograms (*C*, *D*) derived from G11 cells [expressing Cx43 with S to A substitutions at 255, 279, 282 (Cx43-S255,279,282A)] in the absence (*A*, *C*) and presence (*B*, *D*) of 100 ng/ml EGF. Records were notch filtered and low-pass filtered at 100 Hz (8-pole Bessel). Calibration bars in *A* and *B* correspond to 2 pA and 2 s and are located near the zero current level. Note the absence of any differences in channel amplitude in the presence vs. absence of EGF.

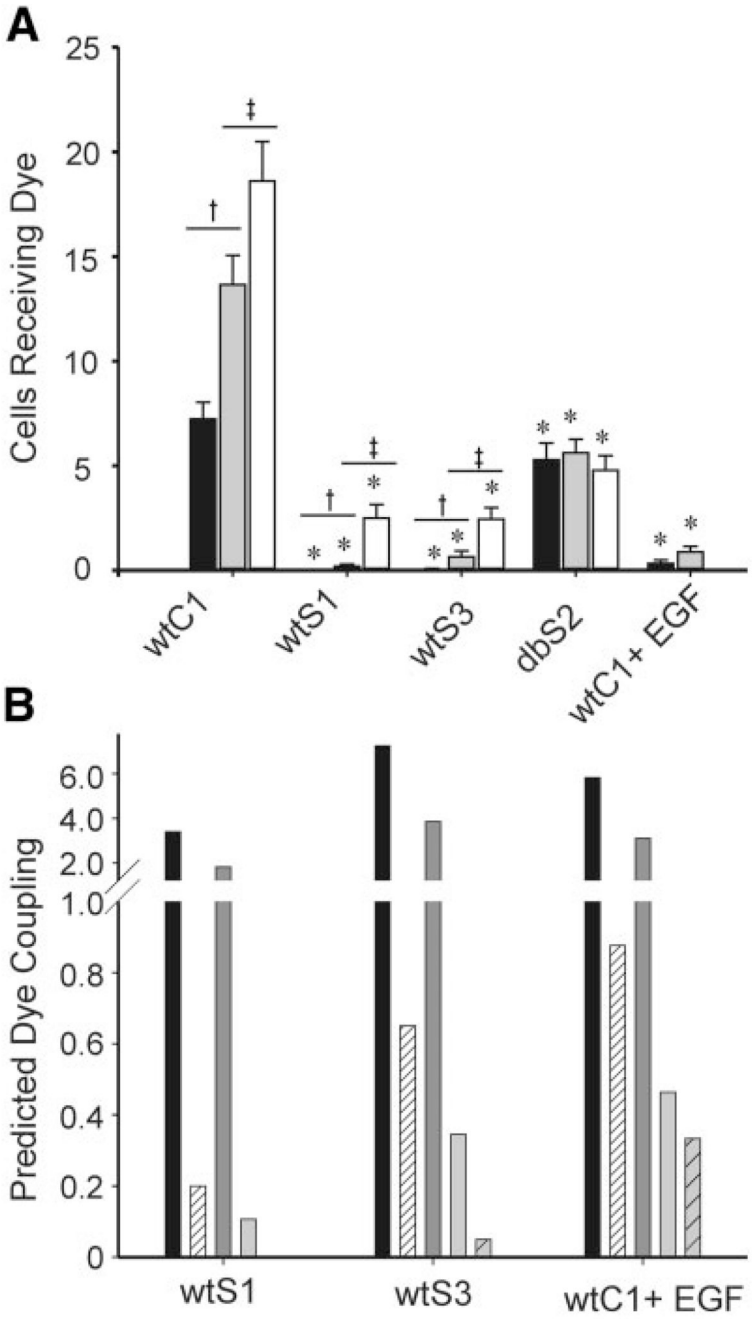

Fig. 5.

Extent of dye coupling (*A*) and expected dye coupling (*B*) for wtC1, wtS1, wtS3, dbS2, and wtC1-EGF-treated cells. A: cells were injected with Lucifer yellow (filled bars), [2-(4-nitro-2,1,3-benzoxadiol-7-yl)aminoethyl]trimethylammonium (NBD-TMA; gray bars), or NBD-TMA after preincubation with 10 μM PP2 media (open bars). wtS1, wtS3, and wtC1 +EGF cells displayed a significant decrease in GJC compared with wtC1 cells. GJC was significantly improved in wtS1 and wtS3 cells after incubation in PP2. The Cx43-Y247,265F mutations in dbS2 cells prevented v-Src-induced dye uncoupling between these cells. *Significant difference from wtC1; † significant difference between Lucifer yellow and NBD-TMA treatments; ‡ significant difference between NBD-TMA and NBD-TMA + PP2

treatments ($P < 0.05$). *B*: filled bars represent the expected level of coupling assuming that NBD-TMA dye coupling decreased in parallel with the decrease in junctional conductance (electrical coupling) observed in Fig. 1. Hatched bars represent the observed level of NBD-TMA coupling reproduced from *A*. Dark gray and light gray bars represent the expected levels of coupling assuming that Lucifer yellow coupling decreased in parallel with the decrease in junctional conductance (dark gray) or NBD-TMA coupling (light gray). Hatched gray bar is the observed level of Lucifer yellow coupling reproduced from *A*. In all cases, the observed levels of coupling were considerably lower than the expected levels of coupling, regardless of the predictor used.